Electronic Supporting Information for:

Geochemical evidence for the application of nanoparticulate colloidal silica gel for in-situ containment of legacy nuclear wastes

Pieter Bots,[*a] Joanna C. Renshaw,[a] Timothy E. Payne,[b] M. Josick Comarmond,[b] Alexandra E.P. Schellenger,[a] Matteo Pedrotti,[a] Eleonora Calì[c] and Rebecca J. Lunn[a]

[a.] *Department of Civil and Environmental Engineering, University of Strathclyde, Glasgow, G1 1XJ, United Kingdom. E-mail: pieter.bots@strath.ac.uk*

[b.] *Australian Nuclear Science and Technology Organisation, Lucas Heights, NSW 2234, Australia.*

[c.] *Department of Materials, Imperial College London, London, SW7 2AZ, United Kingdom.*

Electronic supplementary information with 7 pages, 5 tables and 1 figure.

Supporting methods

Transmission Electron Microscopy

The colloidal silica nanoparticles, and the gelling of the colloidal silica with 1.4 M NaCl and with 0.175 M $CaCl_2$ in the accelerant were imaged using transmission electron microscope (TEM). Gelling of colloidal silica was induced by mixing 5 ml of colloidal silica with 1 ml of either 1.4 M NaCl or 0.175 M $CaCl_2$. During the gelling process (prior to complete gelling of the colloidal silica) two samples were taken from both samples (after ~10 minutes and after ~1 hour). Aliquots of these four samples and an aliquot of the colloidal silica were diluted 1000 and sonicated briefly, to prevent aggregation. The samples were subsequently drop-casted onto a holey carbon film supported by a copper grid (TAAB) and air dried (overnight) prior to analyses. These air dried samples were imaged using a Jeol 2100F TEM operated at 200 kV.

Adsorption

To produce contaminated solid samples (with compositions described in Table S1) for subsequent leaching experiments, adsorption experiments were performed at pH 7, and a solid loading of 10 g/l, in simulated groundwater (10 mM NaCl). 0.25 g of the solid mixture was weighed in a 50 ml polypropylene centrifuge tubes. Next approximately 22 ml of 10 mM NaCl was added to the centrifuge tubes. The solids and solutions were homogenized and the pH was adjusted to pH 7 using small aliquots of 10 mM NaOH. These mixtures were agitated on a shaker for at least 20 hours, after which the pH values were checked. pH adjustments and agitation on a shaker were repeated until the pH values were stable, after which the volumes in the centrifuge tubes were corrected (by weight) up to 25 ml using 10 mM NaCl. To produce soil/waste mixtures (Table S1) with environmentally relevant trace Sr and Cs contamination, soil/waste suspensions were spiked using slightly acidified radiotracer stock solutions (5 kBq/ml Sr-85 and Cs-137) to obtain trace concentrations of 20 Bq/ml Sr-85 ($2.7 \cdot 10^{-10}$ mM Sr) and Cs-137 ($4.6 \cdot 10^{-8}$ mM Cs) in these adsorption experiments. To produce solids (for all 3 mixtures of solids, Table S1) with elevated Sr and Cs contamination (for direct comparison with XAS analyses), suspensions were spiked using slightly acidified 10,000 ppm Sr and Cs stock solution to obtain concentrations of 25 ppm Sr and Cs (0.29 mM Sr and 0.19 mM Cs) in these adsorption experiments. After spiking the suspensions, an aliquot of a 10 mM NaOH solution was added to counter acidification from the stock solutions. These adsorption experiments were equilibrated for 48 hours, after which the pH was measured, the suspensions were centrifuged at 8,000 rpm for 20 minutes, 10 ml of the solution samples were obtained for aqueous analyses and the contaminated solids were separated from the supernatant. The contaminated solids were separated from the supernatant by decanting the remainder of the supernatant and the contaminated solid was dried in an oven at 70°C for 72 hours to remove any remaining liquid from the contaminated solid, to prevent diluting the colloidal silica gel.

Table S1. The composition of the model solids (soil, waste, and soil-waste mixtures) used to create the contaminated solids for the leaching experiments.

Solid/mineral	Soil Weight %	Waste Weight %	Soil/waste Weight %
Quartz	45	-	22.5
Illite-smectite	25	-	12.5
Kaolinite	25	-	12.5
Goethite	3	-	1.5
Anatase	2	-	1
PVC	-	40	20
Cellulose	-	20	10
Magnetite	-	20	10
Gibbsite	-	20	10

The solution samples (10 ml) of the adsorption experiments at trace Sr and Cs concentrations (20 Bq/ml) were acidified (with 0.1 ml concentrated HCl) prior to γ-spectroscopy for the concentrations of Sr-85 and Cs-137 (ORTEC P-type high purity germanium detector coupled to ORTEC DSPec Pro digital spectrometers) and subsequent ICP-AES for the concentration of Na (Varian Vista AES) analyses. The half-life of Sr-85 (64.84 days) and Cs-137 (30.17 years) was used to subsequently correct the activity concentrations of Sr-85 and Cs-137 to correspond to the start of the adsorption experiments to enable accurate calculation of the Sr and Cs retention on the solid. Hence all the reported activities and activity concentrations correspond to the initial activity in the adsorption experiments. The solutions samples of the adsorption experiments at elevated Sr and Cs concentrations (25 ppm) were filtered through 0.2 µm PVDF syringe filters for subsequent analyses using cation chromatography for the concentrations of Sr, Cs and Na (Metrohm CatAn Professional IC with a C6 cation exchange column and an eluent containing 4.5 mM HNO_3 and 1.5 mM dipicolinic acid). The results from these aqueous analyses were used to calculate the solid Sr and Cs concentrations and the respective distribution coefficients (K_D values), summarized in Table S2.

Table S2. Description of the contaminated solids used in the experimental work.

Matrix/ description	Sr and Cs content and K_D of the samples contaminated during adsorption experiments at pH 7 and trace concentrations of Sr-85 and Cs-137 (20 Bq/ml)^				K_D values from desorption experiments in DI^		K_D values from desorption experiments in 10 mM NaCl^	
	Sr-85 (kBq/g)	Sr-85 K_D (ml/g)	Cs-137 (kBq/g)	Cs-137 K_D (ml/g)	Sr-85 K_D (ml/g)	Cs-137 K_D (ml/g)	Sr-85 K_D (ml/g)	Cs-137 K_D (ml/g)
Soil	1.8	306	2.3	1891	-	-	-	-
Waste	1.1	89	0.5	27	-	-	-	-
Soil/waste*	1.5(1)	171(30)	2.2(1)	1091(448)	5189(425)	2652(470)	450(64)	6990(2322)
	Sr and Cs content and K_D of the samples contaminated during adsorption experiments at pH 7 and elevated concentrations of Sr and Cs (25 ppm)^				**K_D values from desorption experiments in DI^**		**K_D values from desorption experiments in 10 mM NaCl^**	
	Sr (mg/g)	Sr K_D (ml/g)	Cs (mg/g)	Cs K_D (ml/g)	Sr K_D (ml/g)	Cs K_D (ml/g)	Sr K_D (ml/g)	Cs K_D (ml/g)
Soil*	1.02(8)	68(9)	0.59(3)	30(2)	30862(15258)	943(269)	326(26)	176(14)
Waste*	0.20(3)	9(1)	0.04(3)	2(1)	165(26)	50(12)	57(5)	31(2)
Soil/waste*	0.58(6)	30(4)	0.31(4)	14(2)	3030(7)	261(4)	135(12)	79(5)
Soil XAS$^{\$}$	-	-	0.84(6)	50(4)	-	-	-	-
Soil/waste XAS$^{\#}$	0.71(5)	38(4)	-	-	-	-	-	-

^ Errors on the solid concentrations of Sr and Cs and the respective K_D values are given in parenthesis and the standard deviation of ≥ 8 adsorption experiments or two subsequent desorption steps

* The Sr and Cs contaminated solid samples treated with colloidal silica gel for leaching and desorption experiments

$^{\$}$ Contamination of soil sample for XAS analyses with only Cs at 25 ppm in solution

$^{\#}$ Contamination of soil/waste sample for XAS analyses with only Sr at 25 ppm in solution

Leaching and desorption experiments

In order to test the impacts of colloidal silica materials (and the type of accelerant used to gel the colloidal silica) on the mobility of Sr and Cs, the contaminated samples (denoted with asterisks in Table S2) were embedded in colloidal silica gel. The dried contaminated samples (Table S2) were mixed with 5 ml of colloidal silica (CS: MP 325, BASF) and with 1 ml of either 1.4 M NaCl [Na-CS] or 0.175 M $CaCl_2$ [Ca-CS] as accelerant (to induce gelling) within the centrifuge tube in which the adsorption experiments were performed (to minimize radiological risks during the experimental set-up, and loss of contaminated materials during transfer). These mixtures of colloidal silica and the contaminated solids were thoroughly mixed using a vortex mixer until relatively homogenous and cured for 7 days to ensure complete gelling of the colloidal silica and equilibrium between the silica porewater geochemistry and the contaminated solids.

After curing the contaminated samples in colloidal silica the leaching procedures were initiated by adding 20 ml of simulated groundwater (10 mM NaCl) to the centrifuge tubes as the leaching supernatant (Fig. 6A). To approximate the long-term conditions of a potential colloidal silica gel barrier (e.g. interaction with continuously flowing uncontaminated groundwater), 10 ml of the leaching supernatant was replaced for 10 ml uncontaminated 10 mM NaCl 20 times over a period of four weeks [4wk]. Additionally, to explore rate effects and equilibrium behaviour, 20 ml of the leaching supernatant for one set of samples at trace Sr and Cs contamination was replaced for 20 ml uncontaminated 10 mM NaCl 10 times over a period of 6 months [6mth]. The 4wk and 6mth leaching experiments at the environmentally relevant trace Sr and Cs contamination were kept open to the atmosphere throughout the experimental duration to simulate environmental conditions. The 4wk leaching experiments at elevated Sr and Cs contamination were only exposed to the atmosphere while replacing the supernatant to limit continuous ingress of CO_2 (throughout the experiment) and minimize the opportunity for $SrCO_3$ precipitation at elevated Sr concentrations. This methodology resulted in 10 leaching experiments, which are summarized in Table S3. Each time the leaching solution was replaced with uncontaminated 10 mM NaCl, the pH was measured and the contaminated supernatant removed from the experiments was analysed for Sr, Cs, Na and Ca using γ-spectroscopy and ICP-AES, or IC as described for the adsorption experiments. Finally, for direct comparison to determine the impacts of colloidal silica gel on Sr and Cs geochemistry, a set of parallel equilibrium desorption experiments were performed on contaminated solid samples in the absence of colloidal silica (Table S3) using deionised water (18.2 MΩ, DI) or 10 mM NaCl as the desorption solution. These desorption experiments were run for two weeks and 10 ml of the contaminated supernatant was replaced twice with uncontaminated DI or 10 ml of the contaminated supernatant was replaced twice with uncontaminated 10 mM NaCl (after 1 and 2 weeks, Table S3). Aliquots of the contaminated supernatant were sampled and analysed as described for the leaching and adsorption experiments, above.

Table S3. Summary of the conditions used during the leaching and parallel equilibrium desorption experiments, the description of the contaminated solid refers to the composition of the solid materials (Table S1) and the respective level of contamination in kBq/g or mg/g as calculated from the results from the adsorption experiments (Table S2).

Description of contaminated solid	Accelerant to initiate colloidal silica gelling	Composition of leaching or desorption solution	Frequency and volume of replacing supernatant / sampling, and duration of experiment	Location of experiment and analyses*
soil/waste; 2.2 kBq/g Cs-137 + 1.5 kBq/g Sr-85	1.4 M NaCl; – Na-CS	10 mM NaCl	10 ml, 20 times, 4 weeks	ANSTO
soil/waste; 2.2 kBq/g Cs-137 + 1.5 kBq/g Sr-85	0.175 M $CaCl_2$; – Ca-CS	10 mM NaCl	10 ml, 20 times, 4 weeks	ANSTO
soil/waste; 2.2 kBq/g Cs-137 + 1.5 kBq/g Sr-85	1.4 M NaCl; – Na-CS	10 mM NaCl	20 ml, 10 times, 6 months	ANSTO
soil/waste; 2.2 kBq/g Cs-137 + 1.5 kBq/g Sr-85	0.175 M $CaCl_2$; – Ca-CS	10 mM NaCl	20 ml, 10 times, 6 months	ANSTO
soil/waste; 2.2 kBq/g Cs-137 + 1.5 kBq/g Sr-85	No colloidal silica gel	DI	10 ml, twice, 2 weeks	ANSTO
soil/waste; 2.2 kBq/g Cs-137 + 1.5 kBq/g Sr-85	No colloidal silica gel	10 mM NaCl	10 ml, twice, 2 weeks	ANSTO
soil/waste; 0.31 mg/g Cs + 0.58 mg/g Sr	1.4 M NaCl; – Na-CS	10 mM NaCl	10 ml, 20 times, 4 weeks	UoS
soil/waste; 0.31 mg/g Cs + 0.58 mg/g Sr	0.175 M $CaCl_2$; – Ca-CS	10 mM NaCl	10 ml, 20 times, 4 weeks	UoS
soil/waste; 0.31 mg/g Cs + 0.58 mg/g Sr	No colloidal silica gel	DI	10 ml, twice, 2 weeks	UoS
soil/waste; 0.31 mg/g Cs + 0.58 mg/g Sr	No colloidal silica gel	10 mM NaCl	10 ml, twice, 2 weeks	UoS
waste; 0.04 mg/g Cs + 0.20 mg/g Sr	1.4 M NaCl; – Na-CS	10 mM NaCl	10 ml, 20 times, 4 weeks	UoS
waste; 0.04 mg/g Cs + 0.20 mg/g Sr	0.175 M $CaCl_2$; – Ca-CS	10 mM NaCl	10 ml, 20 times, 4 weeks	UoS
waste; 0.04 mg/g Cs + 0.20 mg/g Sr	No colloidal silica gel	DI	10 ml, twice, 2 weeks	UoS
waste; 0.04 mg/g Cs + 0.20 mg/g Sr	No colloidal silica gel	10 mM NaCl	10 ml, twice, 2 weeks	UoS
soil; 0.59 mg/g Cs + 1.02 mg/g Sr	1.4 M NaCl; – Na-CS	10 mM NaCl	10 ml, 20 times, 4 weeks	UoS
soil; 0.59 mg/g Cs + 1.02 mg/g Sr	0.175 M $CaCl_2$; – Ca-CS	10 mM NaCl	10 ml, 20 times, 4 weeks	UoS
soil; 0.59 mg/g Cs + 1.02 mg/g Sr	No colloidal silica gel	DI	10 ml, twice, 2 weeks	UoS
soil; 0.59 mg/g Cs + 1.02 mg/g Sr	No colloidal silica gel	10 mM NaCl	10 ml, twice, 2 weeks	UoS

*ANSTO: Australian Nuclear Science and Technology Organisation (NSW, Australia); UoS: University of Strathclyde (Scotland, UK).

Data Treatment.

First of all, the similarities between the experiments performed separately at the collaborating institutions (Table S3), specifically with respect to the analysed Na concentrations (Fig. 2d and h) highlights the reproducibility of the experimental setup.

Fig. 6 summarizes the leaching experimental set-up (A) and an overview of the potential processes affecting the leaching and mobility of Sr and Cs and the equilibration of the leaching solution with the colloidal silica porewater (B-D). Fig. 6D represents the immobilization capacity of the soil and waste minerals with respect to Sr^{2+} and Cs^{+} using illite as an example through: (i) diffusion and subsequent trapping of cations in the interlayer of mica (e.g. illite) and smectite (e.g. montmorillonite) group clay minerals;[1] (ii) inner-sphere surface complexation, where an ion complexes directly with the surface of the (clay) minerals without an H_2O molecule between the cation and the surface; (iii) outer-sphere surface complexation, where an ion interacts with (clay) mineral surfaces with fully hydrated cations, predominantly through electrostatic forces; and (iv) labile ions in the diffuse layer where the charge of the (clay) mineral surface causes gradients in the concentration of ions and thus only exert a weak force on the cations of interest.[2] Fig. 6C represents the diffusion of ions through the porewater within the gelled colloidal silica (a) and the adsorption and desorption (b) processes (through inner- and/or outer-sphere surface complexation and within the diffuse layer affecting the effective rate of diffusion of ions through the colloidal silica as visualized in Fig. 6D). The processes described in Fig. 6D and C, are applicable to and can affect the mobility of Sr, Cs, Na, Ca and OH^-. Additionally, Na and Ca (from the colloidal silica and the accelerant) and the pH of the porewater can affect the availability of complexation sites for Sr and Cs (and other radionuclides of interest). This can subsequently affect the immobilization capacity of the (clay) minerals and of silica nanoparticles for Sr and Cs (and other radionuclides of interest). Fig. 6B represents the overall leaching process of Na, Ca, Sr, Cs and OH from the contaminated sample embedded in a colloidal silica matrix into the leaching solution (10 mM NaCl) impacted by the processes described in Fig. 6D and C. Fig. 6A shows a schematic of the overall experimental setup and the equilibration of the leaching solution with atmospheric CO_2 from the headspace of the experiment. The diffusion of CO_2 into the leaching solution and subsequently into the colloidal silica porewater and the diffusion of OH^- from the colloidal silica porewater into the leaching solution will impact on the pH of the leaching solution and the colloidal silica porewater.

Sorption of Sr and Cs to solid materials shows hysteresis, resulting in different distribution coefficients during the adsorption and desorption of Sr and Cs.[1, 3, 4] This is also apparent in the presented distribution coefficients (Table S2; e.g. distribution coefficients (K_D) for Cs interaction with simulated soil/waste mixture at 20 Bq/ml are $1{\cdot}10^3$ and $7{\cdot}10^3$ ml/g as determined from the results from the adsorption and desorption experiments, respectively). To account for this hysteresis, we compare the apparent K_D values determined from the aqueous Sr and Cs concentration during our leaching experiments to distribution coefficients calculated from desorption experiments (Table S2), rather than the distribution coefficients calculated from the adsorption experiments to produce the contaminated solids. To enable the comparison of the (apparent) Sr and Cs K_D values with the K_D values from the desorption experiments the apparent K_D values were calculated using the aqueous Sr and Cs concentrations. The Sr and Cs concentrations

were used to calculate the mass or activity of Sr and Cs retained in the contaminated solid sample embedded in colloidal silica (Na-CS and Ca-CS). These values were then divided by the mass of the contaminated sample to calculate the solid Sr or Cs concentration within the samples embedded in colloidal silica gel (in Bq/g or ppm; assuming all Sr and Cs within the samples was retained on the original solid). Then the solid Sr and Cs concentrations were divided by the aqueous Sr or Cs concentration in (Bq/ml or ppm; Equation 1). By calculating the apparent distribution coefficient (K_D) values by (incorrectly) assuming all Sr and Cs were retained on the original solid samples, any impact of the colloidal silica gel will become apparent: (1) if the colloidal silica gel has negligible impact on the speciation or mobility of Sr or Cs, the apparent K_D values should be identical to the K_D values calculated from the desorption experiments; (2) if the colloidal silica gel has a positive or negative impact on the speciation or mobility of Sr or Cs, the apparent K_D values should either increase or decrease (respectively) compared to the K_D values calculated from the desorption experiments. Hence, Fig. 2b,c,f and g include the K_D values calculated from the parallel desorption experiments inform on the impacts of colloidal silica on the mobility of Sr and Cs. Furthermore, the apparent K_D values will be affected by all the processes visualized in Fig. 6, and are corrected for the removal of Sr and Cs from the system during the sampling regimes. Consequently, if the apparent K_D reaches a stable value, either equilibrium or a steady-state has been reached. By comparing the K_D values between the two experiments at trace Sr and Cs contamination with different sampling regimes (4wk vs. 6mth) a steady state can be distinguished from an equilibrium (e.g. if equilibrium is reached in the 4wk experiments, the apparent K_D values should be identical to the apparent K_D values from the corresponding 6mth). Because of the different length and timescales a full-sized colloidal silica barrier will exhibit, this comparison between the 4wk and 6mth experiments could furthermore provide clues on the impact of variations in the flow rate of uncontaminated groundwater around a potential colloidal silica barrier.

$$K_D = \frac{[Sr]_{solid-silica\ gel}}{[Sr]_{aqueous}}; K_D = \frac{[Cs]_{solid-silica\ gel}}{[Cs]_{aqueous}} \qquad \textbf{Equation 1}$$

X-ray absorption spectroscopy

Leaching Experiments to produce XAS samples. X-ray absorption spectroscopy (XAS), and specifically analyses of the extended x-ray absorption fine structure (EXAFS) spectra is a powerful tool to determine the speciation of contaminants, including the respective mobility and bioavailability, and the impacts of environmental engineering strategies on the speciation of contaminants.[5, 6] To enable the development of a comprehensive conceptual model on the impacts of colloidal silica on the mobility and leaching potential of Sr and Cs (Fig. 6), additional experiments were performed to analyse the impacts of colloidal silica on the speciation Sr and Cs with synchrotron based X-ray absorption spectroscopy (XAS). 0.4 g of the contaminated samples were prepared using the same procedure as for the adsorption experiments described above and Table S1 and Table S2. However, preliminary experiments indicate competition between Sr and Cs for adsorption on soil minerals, so the solids for XAS analyses were contaminated with Sr or Cs separately in order to increase their solid concentration and subsequently to improve the XAS signal. Furthermore, because the adsorption experiments showed that none of the waste materials significantly adsorbed Cs (Table S2), the soil mixture was used for the contaminated solids for Cs XAS analyses while the soil/waste mixture was used to produce the contaminated solids for Sr XAS analyses. Aliquots of the contaminated solids (Table S2 and Table S4) were loaded into 4 ml cryo-centrifuge tubes and stored at -80°C prior to XAS analyses. The leaching experiments on the contaminated solids were further adjusted to prevent diluting the Sr or Cs content below the detection limit for XAS analyses by decreasing the amount of colloidal silica gel used (0.31 ml of colloidal silica and 0.06 ml of accelerant). Additionally, the contaminated solid, colloidal silica gel and accelerant were mixed within 4 ml cryo-centrifuge tubes (for (in-situ) XAS analyses) and cured for a week prior to leaching experiments.

Table S4. Description of the experiments and resulting samples, including the standards prepared for X-ray absorption spectroscopy analyses.

Description of contaminated solid	Accelerant to initiate colloidal silica gelling	Description of resulting sample
Soil; 0.84 mg/g Cs	No colloidal silica	Initial contaminated soil
Soil; 0.84 mg/g Cs	1.4 M NaCl	t = 0 days; prior to leaching/equilibration
Soil; 0.84 mg/g Cs	1.4 M NaCl	t = 20 days; after leaching/equilibration
Soil; 0.84 mg/g Cs*	0.175 M $CaCl_2$	t = 0 days; prior to leaching/equilibration
Soil; 0.84 mg/g Cs*	0.175 M $CaCl_2$	t = 20 days; after leaching/equilibration
None	No colloidal silica	Standard: 10,000 ppm Cs^+ (as CsCl), 10 mM HCl
None	0.8 M CsCl	Standard: Cs in gelled colloidal silica
Soil/waste; 0.71 mg/g Sr	No colloidal silica	Initial contaminated soil/waste
Soil/waste; 0.71 mg/g Sr	1.4 M NaCl	t = 0 days; prior to leaching/equilibration
Soil/waste; 0.71 mg/g Sr	1.4 M NaCl	t = 20 days; after leaching/equilibration
Soil/waste; 0.71 mg/g Sr	0.175 M $CaCl_2$*	t = 0 days; prior to leaching/equilibration*
Soil/waste; 0.71 mg/g Sr	0.175 M $CaCl_2$*	t = 20 days; after leaching/equilibration*
None	No colloidal silica	Standard: 10,000 ppm Sr^{2+} (as $SrCl_2$), 10 mM HCl
None	No colloidal silica	Standard: $SrCO_3$
None	0.2 M $SrCl_2$	Standard: Sr in gelled colloidal silica

* denotes samples that were analyzed for XANES only

To induce leaching / equilibration with simulated groundwater (10mM NaCl), the 4 ml cryo-centrifuge tubes containing the contaminated solid – silica gel mixtures (Table S4) were suspended in 40 ml 10 mM NaCl in a 50 ml centrifuge tube for 20 days. 2.5 ml aliquots of the simulated groundwater were sampled after 1, 3, 7, 14 and 20 days using a syringe and filtered through a 0.2 µm PVDF syringe filter for analyses using cation chromatography. After 20 days the 4 ml cryo-vials containing the leached/equilibrated samples were removed from the simulated groundwater and stored at room temperature (to prevent the formation of ice crystals damaging the colloidal silica gel) prior to XAS analyses. Finally, several standards were prepared for XAS analyses (Table S4), including colloidal silica gelled with 0.8 M CsCl and with 0.2 M $SrCl_2$ to inform on the speciation of Sr and Cs within colloidal silica.

XAS analyses. X-ray absorption spectroscopy was performed at the general purpose XAS beamline (B18) at Diamond Light Source.[7] The Ti K-edge (4,966 eV) interferes with the Cs L_3-edge (5,012 eV) and the Cs L_3-edge exhibits several strong multi-electron photoexcitation features in the Cs L_3-edge EXAFS spectra.[8, 9] To avoid resulting complications in XANES analyses and EXAFS fitting, Cs XAS was performed on the Cs K-edge (35,985 eV) rather than the L_3-edge.[10-12] Cs K-edge spectra were collected using a Si(311) monochromator and Sr K-edge (16,105 eV) spectra were collected using a Si(111) monochromator. The energy of the X-rays was calibrated using an yttrium foil (for the Sr K-edge) and an antimony foil (for the Cs K-edge). The samples were analysed for their spectra in fluorescence mode using a 36-element Ge detector, and the standards were analysed for their spectra in transmission mode. The samples, and the colloidal silica (CS) and $SrCO_3$ standards were measured at liquid nitrogen temperature (80 K) in a LN2 cryostat, while the aqueous standards (10,000 ppm Cs^+ and Sr^{2+}) were analysed at room temperature. The collected spectra were processed and analysed using the Demeter software package.[13] Athena was used for data reduction and background subtraction. Artemis was used to fit the Fourier Transform (in R-space) of the EXAFS spectra. FEFF6[14] was used to calculate the (initial) Sr and Cs scattering paths using models and subsequent crystallographic information files for Sr and Cs, developed using the illite crystallographic information.[15]

Table S5 Summary of the fit ranges used for the EXAFS fits, and the respective goodness of fit parameters (R-factor, reduced χ^2 and the f-test results).

Sample	k-range ($Å^{-1}$)	R-range (Å)	Paths	No. of variables	R-factor	Reduced χ^2	f-test
Sr in gelled colloidal silica	3-10	1.6-3.5	Sr-O	3	0.0046	594.0	
Soil/waste; 0.71 mg/g Sr	3-10	1.6-4	Sr-O	3	0.0048	147.9	
			Sr-O,Si/Al	5	0.0018	62.5	93.3%
Soil/waste; 0.71 mg/g Sr; Na-CS; t = 0 days	3-10	1.6-4	Sr-O	3	0.0071	365.8	
			Sr-O,Si/Al	5	0.0027	156.3	92.5%
Soil/waste; 0.71 mg/g Sr; Na-CS; t = 20 days	3-10	1.6-4	Sr-O	3	0.0063	288.7	
			Sr-O,Si/Al	5	0.0012	64.8	99.0%
Soil/waste; 0.71 mg/g Sr; Ca-CS; t = 0 days	3-10	1.6-4	Sr-O	3	0.0062	181.3	
			Sr-O,Si/Al	5	0.0035	121.8	78.6%
Soil/waste; 0.71 mg/g Sr; Ca-CS; t = 20 days	3-10	1.6-4	Sr-O	3	0.0072	73.0	
			Sr-O,Si/Al	5	0.0032	33.6	89.4%
Sr^{2+}	3-10	1.6-3.5	Sr-O	3	0.0059	8115	
Cs in gelled colloidal silica	2.5-10	2.2-5.2	Cs-O	3	0.194	655.1	
			Cs-O,Cs	5	0.059	284.1	99.6%
			Cs-O,Cs,Cs	6	0.039	229.8	92.6%
			Cs-O,Si,Cs,Cs	8	0.018	139.1	90.4%
Soil; 0.84 mg/g Cs*	3.5-9	1.8-3.8	Cs-O	7	0.268	277.8	
Soil; 0.84 mg/g Cs; Na-CS; t = 0 days*	3.5-8.5	1.8-3.8	Cs-O,Si/Al	11	0.045	69.2	99.8%
Soil; 0.84 mg/g Cs; Na-CS; t = 20 days*	3.5-9	1.8-3.8	Cs-O,O,Si/Al	14	0.019	33.8	85.0%
Cs^{+}	2.5-9.5	1.7-3.5	Cs-O	3	0.048	217.1	
			Cs-O,O	5	0.004	14.7	97.7%

[#]The statistical confidence that the addition of the scattering path improved the goodness of fit to the EXAFS spectrum/spectra calculated using the f-test for EXAFS[16]

*The σ^2 from the Cs-O scattering paths in all soil samples were simultaneously fitted to the same value and the σ^2 for the Cs-Si/Al scattering paths in all the soil samples were simultaneously fitted to the same value, hence these cannot be separated for the R-factor, the reduced χ^2 and the f-test.

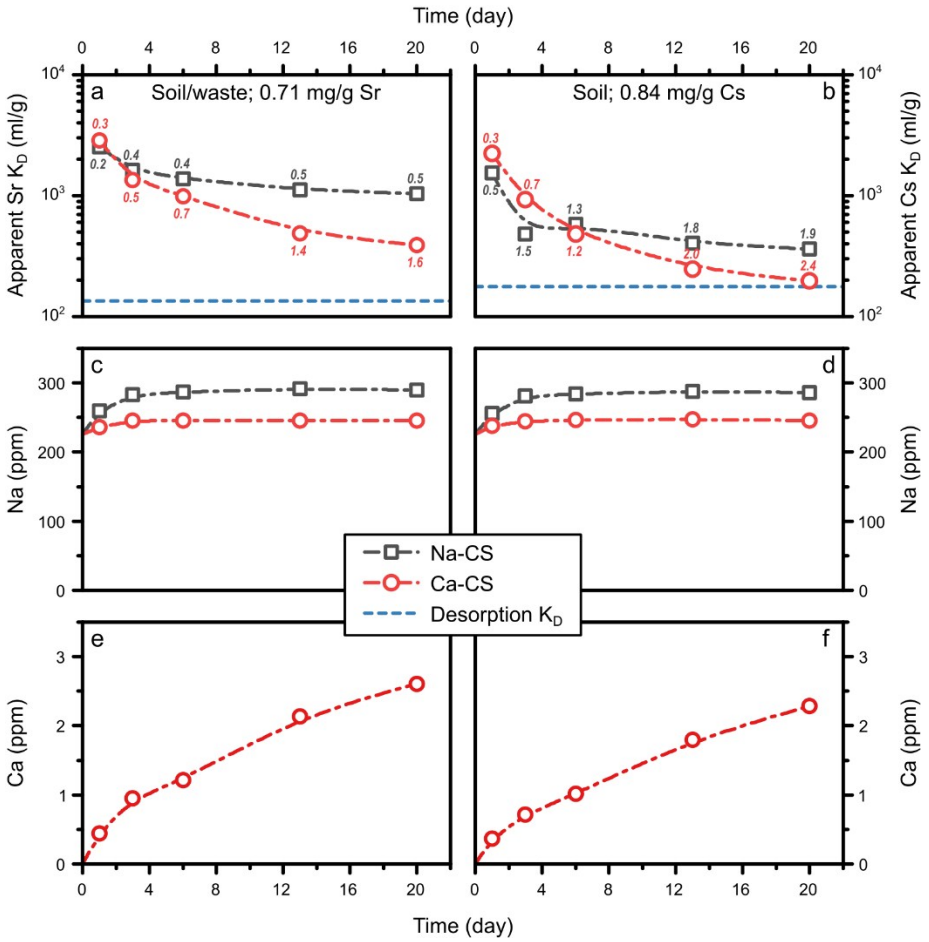

Fig. S1. Summary of the leaching experiments on the soil/waste samples contaminated with 0.71 mg/g Sr (a, c, e) and on the soil samples contaminated with 0.84 mg/g Cs (b, d, f) embedded in colloidal silica gelled with either 1.4 M NaCl (Na-CS) or 0.175 M $CaCl_2$ (Ca-CS) to produce samples for the Sr and Cs K-edge XAS analyses. The apparent Sr and Cs K_D values are plotted (symbols and dash-dotted lines) in conjunction with the parallel desorption K_D values (horizontal dashed line) in a and b; the concentration of Na in the supernatant (resulting from the accelerant and/or the colloidal silica) are plotted in c and d and the Ca concentrations from the accelerant in the Ca-CS experiments are plotted in e and f. The legend refers to the accelerant type used to gel the colloidal silica and the numbers refer to the measured Sr (a) or Cs (b) concentrations in the supernatant (in ppm) used to calculate the apparent K_D values; the final pH in these equilibration experiments are 8.6 (Na-CS) and 8.3 (Ca-CS).

Aqueous results from the leaching experiments to produce XAS samples

The evolution of the apparent Sr and Cs K_D values during these leaching experiments are summarized in Fig. S1a and b. Due to the differences in setup to produce samples suitable for XAS analyses, i.e. without replenishing the supernatant with uncontaminated solutions, the Na concentration within the supernatant increased to 286 ppm Na (12.4 mM Na), or to 246 ppm Na (10.7 mM), during the Na-CS or the Ca-CS leaching experiments, respectively (Fig. S1c and d) and the Ca concentration continuously increased to 2.5 ppm (0.06 mM) during the Ca-CS experiments (Fig. S1e and f). Furthermore, the final pH within the supernatant (and likely within the colloidal silica porewater) was at 8.6 and 8.3, compared to pH 9.5 during the leaching experiments (Fig. 2a and e), due to a lower buffer capacity from a smaller volume of colloidal silica and due to additional CO_2 ingress into the experiment while the supernatant was not replaced for fresh uncontaminated 10 mM NaCl (with a negligible CO_2 content). The apparent Sr K_D values after one day of leaching was $2.5 \cdot 10^3$ ml/g and $2.9 \cdot 10^3$ ml/g (Fig. S1a) in the Na-CS and the Ca-CS leaching experiments, respectively, and the apparent Cs K_D values were $1.5 \cdot 10^3$ ml/g and $2.2 \cdot 10^3$ ml/g (Fig. S1b) in the Na-CS and the Ca-CS leaching experiments, respectively. These initial apparent K_D values are in the same order of magnitude as the initial apparent K_D values in the previous leaching experiments, suggesting that the same/similar processes control the leaching of Sr and Cs in these leaching experiments to produce samples for XAS analyses. Contrary to the previous leaching experiments, the apparent K_D values decreased during the leaching experiments (Fig. S1). This drop in the apparent K_D values was likely caused by less silica sorption sites from a proportionally smaller amount of colloidal silica and a decrease in the pH in the colloidal silica porewater to below the adsorption edge for Sr and Cs adsorption to amorphous silica,[17-19] as indicated by the measured final pH values (8.6 and 8.3) in the supernatant.

References

1. A. J. Fuller, S. Shaw, M. B. Ward, S. J. Haigh, J. F. W. Mosselmans, C. L. Peacock, S. Stackhouse, A. J. Dent, D. Trivedi and I. T. Burke, Caesium incorporation and retention in illite interlayers, *Applied Clay Science*, 2015, **108**, 128-134.
2. G. Sposito, N. T. Skipper, R. Sutton, S. H. Park, A. K. Soper and J. A. Greathouse, Surface geochemistry of the clay minerals, *Proceedings of the National Academy of Sciences of the United States of America*, 1999, **96**, 3358-3364.
3. A. Boyer, P. Ning, D. Killey, M. Klukas, D. Rowan, A. J. Simpson and E. Passeport, Strontium adsorption and desorption in wetlands: Role of organic matter functional groups and environmental implications, *Water Research*, 2018, **133**, 27-36.
4. C. B. Durrant, J. D. Begg, A. B. Kersting and M. Zavarin, Cesium sorption reversibility and kinetics on illite, montmorillonite, and kaolinite, *Science of the Total Environment*, 2018, **610-611**, 511-520.
5. G. E. Brown Jr, A. L. Foster and J. D. Ostergren, Mineral surfaces and bioavailability of heavy metals: A molecular-scale perspective, *Proceedings of the National Academy of Sciences of the United States of America*, 1999, **96**, 3388-3395.
6. K. Maher, J. R. Bargar and G. E. Brown, Environmental Speciation of Actinides, *Inorganic Chemistry*, 2013, **52**, 3510-3532.
7. A. J. Dent, G. Cibin, S. Ramos, S. A. Parry, D. Gianolio, A. D. Smith, S. M. Scott, L. Varandas, S. Patel, M. R. Pearson, L. Hudson, N. A. Krumpa, A. S. Marsch and P. E. Robbins, Performance of B18, the core EXAFS bending magnet beamline at diamond, *Journal of Physics: Conference Series*, 2013, **430**.
8. I. Arčon, A. Kodre, J. Padežnik Gomilšek, M. Hribar and A. Mihelič Cs L-edge EXAFS atomic absorption background, *Physica Scripta T*, 2005, **T115**, 235-236.
9. A. Kodre, I. Arčon, M. Hribar, M. Štuhec, F. Villain, W. Drube and L. Tröger, Strong multielectron absorption effects in the L-edge EXAFS spectra of elements from I to Ce, *Physica B: Physics of Condensed Matter*, 1995, **208-209**, 379-380.
10. B. C. Bostick, M. A. Vairavamurthy, K. G. Karthikeyan and J. Chorover, Cesium adsorption on clay minerals: An EXAFS spectroscopic investigation, *Environmental Science and Technology*, 2002, **36**, 2670-2676.
11. Q. H. Fan, M. Tanaka, K. Tanaka, A. Sakaguchi and Y. Takahashi, An EXAFS study on the effects of natural organic matter and the expandability of clay minerals on cesium adsorption and mobility, *Geochimica et Cosmochimica Acta*, 2014, **135**, 49-65.
12. Q. Fan, N. Yamaguchi, M. Tanaka, H. Tsukada and Y. Takahashi, Relationship between the adsorption species of cesium and radiocesium interception potential in soils and minerals: An EXAFS study, *Journal of Environmental Radioactivity*, 2014, **138**, 92-100.
13. B. Ravel and M. Newville, ATHENA, ARTEMIS, HEPHAESTUS: data analysis for X-ray absorption spectroscopy using IFEFFIT, *Journal of Synchrotron Radiation*, 2005, **12**, 537-541.
14. B. Ravel and J. J. Rehr, Full multiple scattering XANES calculations, *Journal De Physique. IV : JP*, 1997, **7**, C2-229-C222-230.
15. V. Drits, J. Srodon and D. D. Eberl, XRD measurement of mean crystalline thickness of illite and illite/smectite: Reappraisal of the Kubler index and the Scherrer equation, *Clays and Clay Minerals*, 1997, **45**, 461-475.
16. L. Downward, C. H. Booth, W. W. Lukens and F. Bridges, 2007.
17. S. A. Carroll, S. K. Roberts, L. J. Criscenti and P. A. O'Day, Surface complexation model for strontium sorption to amorphous silica and goethite, *Geochemical Transactions*, 2008, **9**.
18. N. Sahai, S. A. Carroll, S. Roberts and P. A. O'Day, X-ray absorption spectroscopy of strontium(II) coordination. II. Sorption and precipitation at kaolinite, amorphous silica, and goethite surfaces, *Journal of Colloid and Interface Science*, 2000, **222**, 198-212.
19. S. Kumar, B. S. Tomar, S. Ramanathan and V. K. Manchanda, Effect of humic acid on cesium sorption on silica colloids.*Journal*, 2006, **94**, 369.